This paper is published as part of a *Dalton Transactions* theme issue:

Dalton Discussion 11: The Renaissance of Main Group Chemistry

Guest Editor: John Arnold
University of California, Berkeley, CA, USA
23 - 25 June 2008

Published in issue 33, 2008, of *Dalton Transactions*

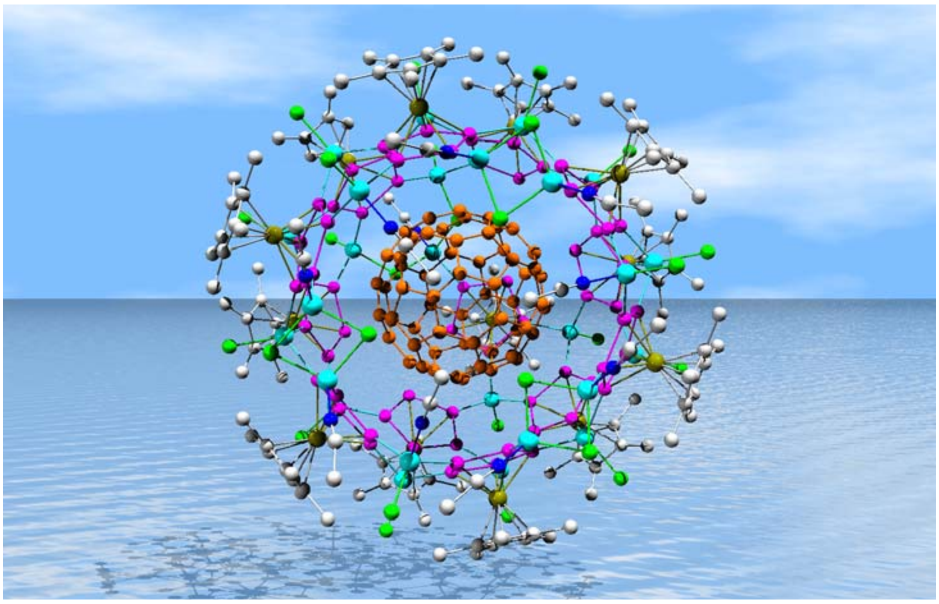

Image reproduced with permission of Manfred Scheer

Papers published in this issue include:

The coordination chemistry of group 15 element ligand complexes—a developing area
Manfred Scheer, *Dalton Trans*., 2008 DOI: 10.1039/b718179p

Formation, structure and bonding of metalloid Al and Ga clusters. A challenge for chemical efforts in nanosciences
Hansgeorg Schnöckel, *Dalton Trans*., 2008 DOI: 10.1039/b718784j

Polymeric materials based on main group elements: the recent development of ambient temperature and controlled routes to polyphosphazenes
Vivienne Blackstone, Alejandro Presa Soto and Ian Manners, *Dalton Trans*., 2008 DOI: 10.1039/b719361k

Recent developments in the chemistry of low valent Group 14 hydrides
Eric Rivard and Philip P. Power, *Dalton Trans*., 2008 DOI: 10.1039/b801400k

Chemistry and physics of silicon nanowire
Peidong Yang, *Dalton Trans*., 2008 DOI: 10.1039/b801440j

Ligand influence on the formation of P/Se semiconductor materials from metal–organic complexes†‡

Arunkumar Panneerselvam,[a] Chinh Q. Nguyen,[a] John Waters,[a] Mohammad A. Malik,[a] Paul O'Brien,*[a] James Raftery[b] and Madeleine Helliwell[b]

Received 6th February 2008, Accepted 3rd April 2008
First published as an Advance Article on the web 23rd July 2008
DOI: 10.1039/b802012d

The complexes $[Ni\{(SeP^iPr_2)_2N\}_2]$ (**1**), $[Ni(Se_2P^iPr_2)_2]$ (**2**), and $[Co(Se_2P^iPr_2)_2]$ (**4**) were synthesised and the X-ray single crystal structures of (**1**) and (**2**) were determined. Thin films of nickel selenide, cobalt selenide and cobalt phosphide have been deposited by the chemical vapour deposition method using imidodiselenophosphinato-nickel(II) (**1**), -cobalt(II) $[Co\{(SeP^iPr_2)_2N\}_2]$ (**3**), diselenophosphinato-nickel(II) (**2**), -cobalt(II) (**4**) and diselenocarbamato-nickel(II) $[Ni(Se_2CNEt_2)_2]$ (**5**), and -cobalt(III) $[Co(Se_2CNEt_2)_3]$ (**6**) precursors.

Introduction

Imidodichalcogenidophosphinato-, dichalcogenidophosphinato- and dichalcogenidocarbamato-metal complexes; $[M\{(EPR_2)_2N\}_2]$, $[M(E_2PR_2)_2]$ and $[M(E_2CNR_2)_2]$, (R = ^{i}Pr, Ph and E = S, Se) and (M = metal atom) have been used as single-source precursors for the deposition of metal chalcogenide thin films by chemical vapour deposition (CVD). Dichalcogenidocarbamato complexes have been studied extensively for the deposition of thin films by metal–organic (MO)CVD and aerosol-assisted (AA)-MOCVD,[1–12] whereas the use of imidodichalcogenidophosphinato-[13–16] or diselenophosphinato-metal[17,18] complexes for the deposition of thin films is more recent. It has been demonstrated that selenocarbamates such as $[M(Se_2CNRR')_2]$[19] (where M = Cd, Zn and R = hexyl, R′ = methyl) are excellent precursors for the synthesis of Group 12 selenides but the synthesis of the diselenocarbamato ligand involves the use of toxic and noxious carbon diselenide. The imidodiselenophosphinato ligand, was prepared by the insertion of elemental selenium into the P–N bond of R_2PNHPR_2.[20] Imidodiphosphinic acid derivatives $R_2P(E)NH(E)PR'_2$ (R, R′ = CH_3, C_6H_5; E = O, S) were first prepared by Schmidpeter *et al.*[21] The synthetic process was improved by Woollins and co-workers to make a wide range of derivatives with R, R′ = Et, ^{i}Pr, ^{t}Bu, OEt, OPh and E = S, Se. A typical synthesis involves two steps, a simple condensation reaction of R_2PCl with $NH(SiMe_3)_2$ to give R_2PNHPR_2 followed by oxidation with O, S or Se. On deprotonation of the amine, the molecule $[R_2P(E)N(E)PR_2]^-$ behaves as a bidentate chelating ligand analogous to acetylacetonate (acac, 2,4-pentanedionato) which can form neutral complexes of the type $[M\{(EPR_2)_2N\}_2]$.[22–27]

Recently we have synthesised a series of diselenophosphinato metal complexes as single-source precursors for the deposition of metal selenide thin films.[17,18] The original method for the preparation of dichalcogenidophosphinato complexes was based on reactions between NaHE (E = S, Se) and $R_2P(E)Cl$.[28–30] This method worked for dithio and thioseleno derivatives but did not give reproducible results for diseleno derivatives. We devised a facile route for the preparation of diselenophosphinate ligands in the form of $(R_2PSe_2)^-$ anions crystallised as alkylammonium salts $(HNEt_3)(R_2PSe_2)$ (R = ^{i}Pr, ^{t}Bu, Ph).[17,18] With a small modification, this method also produced the thioselenophosphinate ligands $[(HNEt_3)^+(R_2PSSe)^-]$ (R = ^{i}Pr, Ph) with high yield and purity. The anions $(R_2PE_2)^-$ (E = S, Se) act as bidentate chelating ligands and readily form complexes with several metals.[18]

The imidodichalcogenidophosphinato, dichalcogenidophosphinato and dichalcogenidocarbamato complexes have four or six-membered ring structures. Several studies have shown that the cleavage of the P–E bond in imidodichalcogenidophosphinato complexes at an appropriate temperature leads to the deposition of metal chalcogenide materials.[15,16,31–34] However our studies have shown that in some cases, the products can be either the metal chalcogenides or phosphides depending upon the nature of the ligand.

Herein the synthesis and characterisation of $[Ni\{(SeP^iPr_2)_2N\}_2]$ (**1**), $[Ni(Se_2P^iPr_2)_2]$ (**2**) and $[Co(Se_2P^iPr_2)_2]$ (**4**) complexes and X-ray single crystal structures of (**1**) and (**2**) are reported. These complexes and $[Co\{(SeP^iPr_2)_2N\}_2]$ (**3**), $[Ni(Se_2CNEt_2)_2]$ (**5**) and $[Co(Se_2CNEt_2)_3]$ (**6**) have been used as single-source precursors to grow metal selenide or phosphide films by AA-MOCVD. A comparative study on the deposition behaviour of the imidodiselenophosphinato-, diselenophosphinato- and diselenocarbamato-nickel and -cobalt complexes is presented.

Results and discussions

The complexes $[Ni\{(SeP^iPr_2)_2N\}_2]$ (**1**), $[Ni(Se_2P^iPr_2)_2]$ (**2**), $[Co\{(SeP^iPr_2)_2N\}_2]$[35] (**3**) and $[Co(Se_2P^iPr_2)_2]$ (**4**) were prepared by direct exchange reactions between the ligands and the metal salts

---

[a] *The School of Chemistry and The School of Materials, The University of Manchester, Oxford Road, Manchester, UK M13 9PL. E-mail: paul.obrien@manchester.ac.uk, azad.malik@manchester.ac.uk; Fax: +44 (0)161 275 4598; Tel: +44 (0)161 275 4652*

[b] *The School of Chemistry, The University of Manchester, Oxford Road, Manchester, UK M13 9PL*

† Based on the presentation given at Dalton Discussion No. 11, 23–25 June 2008, University of California, Berkeley, USA.

‡ CCDC reference numbers 675796, 675797 and 676882. For crystallographic data in CIF or other electronic format see DOI: 10.1039/b802012d

in methanol (eqn (1) and (2)). All of these complexes are crystalline solids and are soluble in common organic solvents. They are stable at room temperature in air over several months.

$$2[{}^{i}\mathrm{Pr_2P(Se)NH(Se)P}{}^{i}\mathrm{Pr_2}] + \mathrm{MCl_2 \cdot 6H_2O} + 2\mathrm{NaOMe} \xrightarrow[\text{for }(\mathbf{1})\text{ and }(\mathbf{3})]{\mathrm{MeOH}} [\mathrm{M\{(SeP}{}^{i}\mathrm{Pr_2)_2N\}_2}] + 2\mathrm{NaCl} \quad (1)$$

$$2[({}^{i}\mathrm{Pr_2PSe_2})(\mathrm{NHEt_3})] + \underset{\mathrm{M=Ni(II),\,Co(II)}}{\mathrm{MCl_2 \cdot 6H_2O}} \xrightarrow[\text{for }(\mathbf{2})\text{ and }(\mathbf{4})]{\mathrm{MeOH}} [\mathrm{M(Se_2P}{}^{i}\mathrm{Pr_2)_2}] + 2(\mathrm{HNEt_3})\mathrm{Cl} \quad (2)$$

X-Ray single crystal diffraction study of [Ni{(SeP^{i}Pr$_2$)$_2$N}$_2$] (1)

[Ni{(SeP^{i}Pr$_2$)$_2$N}$_2$] was crystallised from solution in THF by evaporating at room temperature. The deep red solution gave two types of crystals; dark red and green. This behaviour is consistent with the well known Lifschitz salts.[36–38] Repeated crystallisations of this complex from other solvents such as acetonitrile or toluene produced similar results, despite the variations in solvent polarity. Crystallisation at lower temperature (~ 4 °C) leads to a predominance of green crystals, whilst green crystals were the sole product of crystallisation from a concentrated solution in THF, cooled to −18 °C. It was speculated that crystallisation at higher temperatures might produce red crystals alone; however repeated attempts to obtain crystals at temperatures significantly above room temperature proved unsuccessful.

Crystallographic analysis determined that the compound is present in a tetrahedral form in the red crystals (Fig. 1(a)) and a square planar form in the green crystals (Fig. 1(b)). X-Ray single crystal diffraction studies on the compound in the square planar form indicated the presence of a molecule of water with partial occupancy in the crystal lattice and within a plausible hydrogen bonding contact (2.70 Å) of N1. The water molecule may have come either from the undistilled solvent used for recrystallisation or from the NiCl$_2$·6H$_2$O. Selected bond distances and angles are summarised in Table 1 and crystallographic data are presented in Table 2.

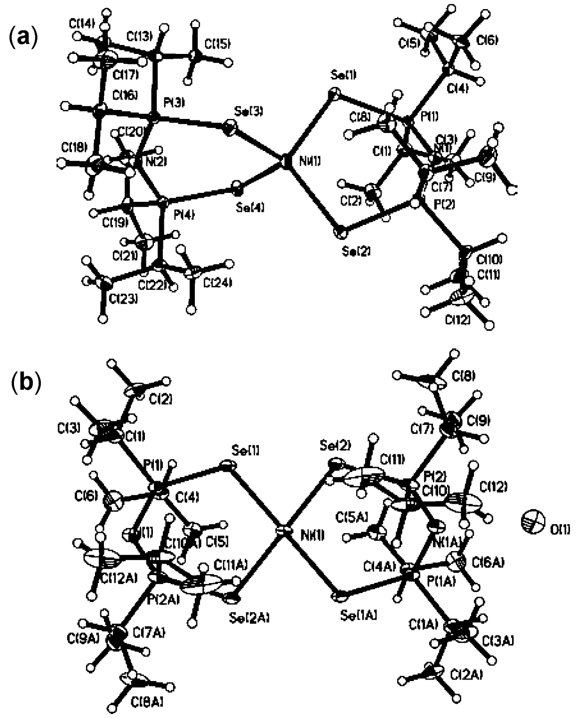

Fig. 1 X-Ray crystal structure of [Ni{(Se$_2$P^{i}Pr$_2$)$_2$N}$_2$], (a) tetrahedral and (b) square planar. In the square planar structure, Ni is on a two-fold axis and it is this two-fold axis acting on the ligand that generates the symmetry related ligand to form the chemical unit.

Several compounds, of the type [M{(EPR$_2$)$_2$N}$_2$] (M = Ni, Pd or Pt; E = S or Se; R = alkyl or Ph), have been reported previously with similar structures.[23,39–43] The literature provides examples of compounds which adopt either square planar or

Table 1 Selected bond lengths (Å) and bond angles (°) for [Ni{(SeP^{i}Pr$_2$)$_2$N}$_2$] and [Ni(Se$_2$P^{i}Pr$_2$)$_2$]

	[Ni{(SeP^{i}Pr$_2$)$_2$N}$_2$]		[Ni(Se$_2$P^{i}Pr$_2$)$_2$]	
	Tetrahedral	Square planar		Square planar
Ni(1)–Se(1)	2.400(1)	2.356(1)	Se(1)–P(1)	2.170(6)
Ni(1)–Se(2)	2.406(1)	2.348(1)	Se(1)–Ni(1)	2.359(3)
Ni(1)–Se(3)	2.405(1)	2.348(1)^a	Se(2)–P(1)	2.173(6)
Ni(1)–Se(4)	2.403(1)	2.356(1)^a	Se(2)–Ni(1)	2.357(3)
N(1)–P(1)	1.593(4)	1.605(3)	Ni(1)–Se(2A)	2.357(3)
N(1)–P(2)	1.597(4)	1.605(3)	Ni(1)–Se(1A)	2.359(3)
N(2)–P(3)	1.595(4)	1.605(3)		
N(2)–P(4)	1.602(4)	1.605(3)		
P(1)–Se(1)	2.190(1)	2.202(1)		
P(2)–Se(2)	2.185(1)	2.188(1)		
P(3)–Se(3)	2.183(1)	2.202(1)^a	P(1)–Se(1)–Ni(1)	84.82(1)
P(4)–Se(4)	2.185(1)	2.188(1)^a	P(1)–Se(2)–Ni(1)	84.83(1)
			Se(2)–Ni(1)–Se(2A)	180
Se(1)–Ni(1)–Se(2)	110.54(3)	101.14(2)	Se(2)–Ni(1)–Se(1A)	90.26(9)
Se(1)–Ni(1)–Se(3)	107.48(3)	78.88(2)	Se(2A)–Ni(1)–Se(1A)	89.74(9)^a
Se(1)–Ni(1)–Se(4)	106.57(3)	178.19(3)	Se(2)–Ni(1)–Se(1)	89.74(9)^a
Se(2)–Ni(1)–Se(4)	108.30(3)	78.88(2)^a	Se(2A)–Ni(1)–Se(1)	90.26(9)
N–P–Se	117.76(2)–118.62(2)	116.18(1)–116.50(1)	Se(1A)–Ni(1)–Se(1)	180
P–Se–Ni	105.97(4)–107.39(4)	108.15(3)–113.47(3)	Se(1A)–Ni(1)–Se(1)	99.99(2)

^{a} Symmetry generated.

tetrahedral geometry in the solid state and compounds such as $[Ni\{(SPMe_2)_2N\}_2]$, show interconversion in solution between tetrahedral and square planar forms.[42] The variation in preferred structure in these cases appears to be based solely on the steric effects relating to the choice and arrangement of alkyl substituents, *e.g.* $[Ni\{(SPPh_2)_2N\}_2]$ is tetrahedral in the solid state probably due to the mutual repulsion of the four bulky phenyl groups, whilst $[Ni\{(SPMe_2)(SPPh_2)N\}_2]$ is square planar with the bulky phenyl groups arranged *cis* to one another.[42] However, $[Ni\{(SeP^iPr_2)_2N\}_2]$ seems to be unique in its class in displaying both square planar and tetrahedral configurations in the solid state. These observations suggests that the steric effects of the isopropyl groups do not confer significantly greater stability to either form, thus both are possible and the assumed geometry is influenced by conditions such as temperature. Both the tetrahedral and square planar forms display similar patterns of bond lengths and angles to their literature analogues.[23,39–43]

X- Ray crystal structure of $[Ni(Se_2P^iPr_2)_2]$ (2)

The diselenophosphinato-nickel complex has a square planar coordination (Fig. 2). The Ni atoms are surrounded by a distorted square of four Se atoms belonging to two bidentate chelating ligands $^iPr_2PSe_2$. The bite angles at the Ni atoms are close to 90°. There is a slight difference in the Ni–Se bond distances which vary from 2.357(3) to 2.359(3) Å.

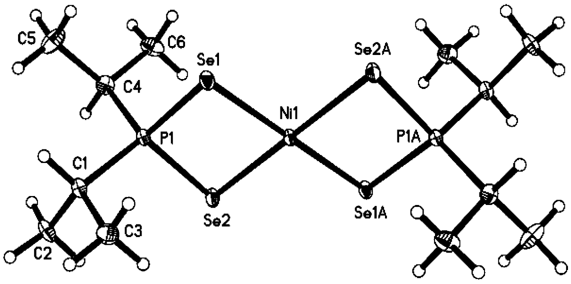

Fig. 2 X-Ray crystal structure of $[Ni(Se_2P^iPr_2)_2]$. The square planar structure is generated from the asymmetric unit by the centre of symmetry upon which the Ni resides.

Differential scanning calorimetry

$[Ni\{(SeP^iPr_2)_2N\}_2]$ (**1**) was studied using differential scanning calorimetry (DSC) and showed an endotherm at 65–120 °C, below the melting point (190–192 °C) of the complex with no accompanying mass loss. The energy associated with the process is very small, it can be assumed to be related to a structural change. Upon retrieval from the DSC apparatus, the sample was found to be semi-plastic in nature and darker in colour, however this state was unstable at room temperature and within minutes the compound reverted to the dark red crystalline form.

Thermogravimetric analysis

Thermogravimetric analysis (TGA) of the nickel and cobalt diselenoimidophosphinato precursors (**1**) and (**3**) revealed a single step decomposition with a weight loss between 261–371 °C and 322–385 °C respectively. The observed final residue (17%) for (**1**) is in fair agreement with the calculated residue (16%) for nickel selenide. For precursor (**3**) the observed residue (5%) is less than the calculated residue (16%) expected for $CoSe_2$ or CoP_2 (10%). XRD analysis of the residue showed the presence of $CoSe_2$ and CoP_2 with some unidentified impurities which may be the reason for the difference between the expected and the observed values. The nickel selenophosphinato precursor (**2**) showed weight loss between 235–298 °C with the observed residue (24%) matching fairly with the calculated residue of (22.5%) for NiSe. The cobalt selenophosphinato precursor (**4**) showed a single step decomposition between 180–312 °C, with the residue matching for $CoSe_2$. The nickel (**5**) and cobalt (**6**) selenocarbamato precursors showed weight loss between 189–305 °C and 271–396 °C respectively. The observed residue for both precursors corresponds to the expected residues for $NiSe_2$ and $CoSe_2$ respectively. XRD analysis of the TGA residues of all compounds other than (**3**) were as expected.

Deposition of nickel selenide films from $[Ni\{(SeP^iPr_2)_2N\}_2]$ (1) by AA-MOCVD

The as-obtained red crystals of the $[Ni\{(SeP^iPr_2)_2N\}_2]$ complex (tetrahedral form) at room temperature was used for AA-MOCVD studies. Deposition was carried out at temperatures 400–500 °C producing uniform black films. XRD studies show in each case, monophasic hexagonal $Ni_{0.85}Se$ (JCPDS 18-0888) with preferred orientation in the (101) direction. The highest peak intensity, and thus the optimum crystallinity, was observed in the film deposited at 450 °C and the peak intensity was seen to diminish progressively with either higher or lower temperatures. SEM studies revealed that the films comprise mixtures of fibrous wires and rods. The morphology of the films change from short, thin wires to thicker and longer wires from lower temperatures (Fig. 3(a),(b)) to higher temperatures (Fig. 3(c),(d)). EDX analysis shows the films contain Ni :Se in a 1 : 1 ratio.

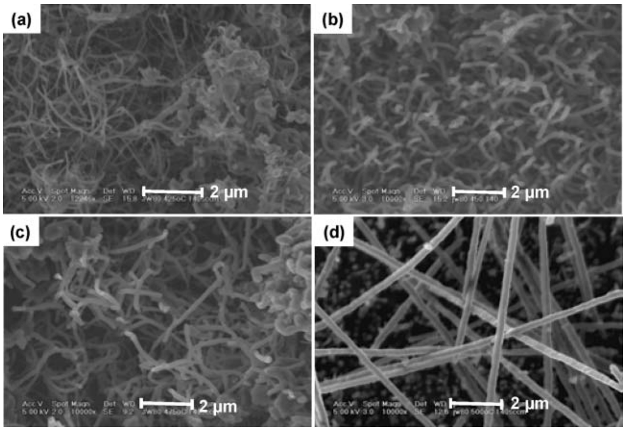

Fig. 3 SEM images of nickel selenide films deposited on glass from $[Ni\{(SeP^iPr_2)_2N\}_2]$ at (a) 425 °C, (b) 450 °C, (c) 475 °C and (d) 500 °C.

Deposition of nickel selenide films from $[Ni(Se_2P^iPr_2)_2]$ (2) by AA-MOCVD

Deposition from $[Ni(Se_2P^iPr_2)_2]$ gave thick black films at 350, 400 and 450 °C. XRD (Fig. 4(a)) results revealed that all films were composed of hexagonal $Ni_{0.85}Se$ (JCPDS 18-0888) with preferred

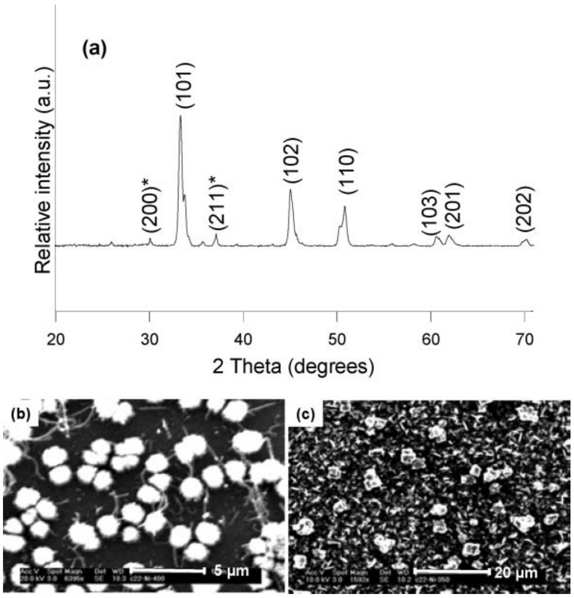

Fig. 4 (a) XRD pattern of nickel selenide film deposited at 400 °C. “*”—NiSe$_2$ peak. SEM images of nickel selenide films deposited on glass from [Ni(Se$_2$P^{i}Pr$_2$)$_2$] at (b) 400 °C and (c) 350 °C.

growth along the (101) plane. Minor peaks for cubic NiSe$_2$ (JCPDS 11-0552) were observed at 2θ values of 30.23 and 36.94°. However, the morphologies analysed by SEM varied from a spherical particles connected by wires at 400 °C (Fig. 4(b)) to a mixture of cubic crystallites and flakes at 350 °C (Fig. 4(c)). EDX analysis shows that the films were selenium rich (61%) with 36% nickel and 3% phosphorus.

Growth of cobalt selenide and cobalt phosphide films from [Co{(SeP^{i}Pr$_2$)$_2$N}$_2$] (3) by AA-MOCVD

Deposition of films was carried out at temperatures 375–525 °C from (**3**) by AA-MOCVD. No deposition occured at 375 °C and a very thin film was deposited at 400 °C which could not be characterised by XRD. Uniform black and partially adherent films were deposited at 425, 450, 475 and 525 °C. XRD of the as-deposited films at 425 and 450 °C showed cobalt selenide films. Surprisingly, the XRD of the as-grown films at 525 and 475 °C revealed the deposition of cobalt selenide and cobalt phosphide films on separate glass substrates depending upon their position in the AA-MOCVD reactor. Cobalt selenide films were deposited on the substrates placed at the beginning of the deposition area of the reactor, which is believed to be at lower temperature than chosen for the film deposition. Cobalt phosphide films were deposited on substrates placed at the centre of the deposition area where the temperature is expected to be highest *i.e.*, at the chosen temperature for film deposition. XRD of the as-deposited cobalt selenide films at all temperatures indicated that they are primarily composed of orthorhombic CoSe$_2$ (JCPDS 10-0408) and cubic Co$_3$Se$_4$ (JCPDS 15–0463), but the predominant growth is along the (111) plane which is the 100% peak of CoSe$_2$ (Fig. 5(a)). Minor peaks corresponding to cubic Co$_9$Se$_8$ (JCPDS 09-0233), cubic CoSe$_2$ (JCPDS 09-0234,“■”); hexagonal Co$_{0.85}$Se (JCPDS 24-0333)[44] and CoSe (JCPDS 15-0464, “□”-unindexed) phases were also observed.

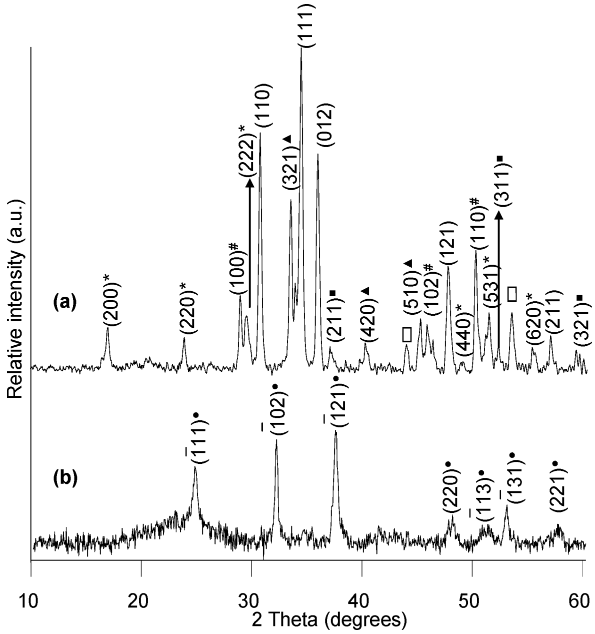

Fig. 5 XRD patterns of (a) cobalt selenide (CoSe$_2$, orthorhombic) and (b) cobalt phosphide (CoP$_2$) films deposited on glass at 525 °C. “*”—Co$_9$Se$_8$, “▲”—Co$_3$Se$_4$, “■”—cubic CoSe$_2$, “#”—Co$_{0.85}$Se and “□”—CoSe, “●”—CoP$_2$ peaks.

SEM images revealed that the films were composed of flakes and wedges at all growth temperatures (Fig. 6(a)–(d)). EDX analysis of the wedge-like features showed that they were composed of 34–36% cobalt and 64–66% selenium with no major phosphorus contamination. The flakes consist of 39–42% cobalt with 55–57% selenium and 3–4% phosphorus.

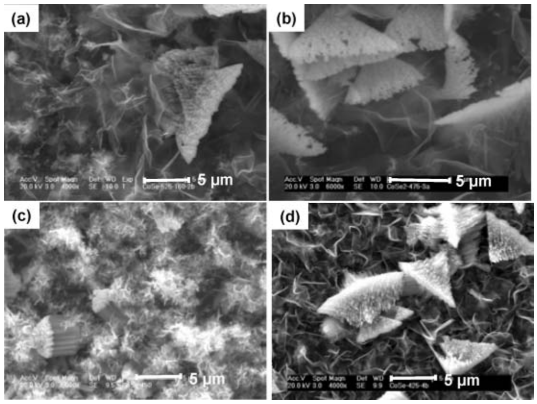

Fig. 6 SEM images of cobalt selenide films deposited on glass from [Co{(SeP^{i}Pr$_2$)$_2$N}$_2$] at (a) 525 °C, (b) 475 °C, (c) 450 and (d) 425 °C.

Cobalt phosphide films were deposited on glass substrates placed at the hottest part of the reactor at 525 and 475 °C. XRD patterns (Fig. 5(b)) of the films grown at 525 °C corresponds to monoclinic CoP$_2$ (JCPDS 77-0263) whereas films deposited at 475 °C showed orthorhombic CoP (JCPDS 29-0497) phase. The morphology of the as-deposited cobalt phosphide films varied from irregular plates at 525 °C to grassy features at 475 °C (Fig. 7(a),(b)). EDX of films deposited at both 525 and 475 °C are cobalt deficient and phosphorus rich with traces of selenium (~ 4%). At 525 °C, the films were composed of 29% cobalt and

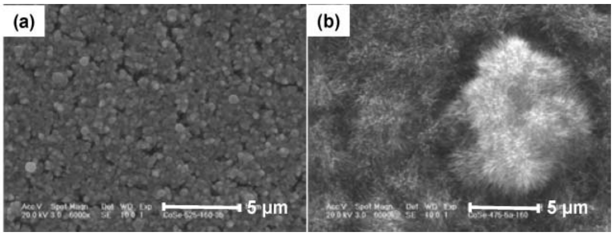

Fig. 7 SEM images of cobalt phosphide films deposited on glass from $[Co\{(SeP^iPr_2)_2N\}_2]$ at (a) 525 °C and (b) 475 °C.

71% phosphorus whereas at 475 °C, the films contain 40% cobalt and 60% phosphorus.

Deposition from $[Co(Se_2P^iPr_2)_2]$ (4) by AA-MOCVD

Deposition from $[Co(Se_2P^iPr_2)_2]$ (**4**) by AA-MOCVD gave thick black films at 450 °C. No deposition was obtained at lower temperatures. The films consist of a mixture of cubic Co_9Se_8 (JCPDS 09-0233) and orthorhombic CoP (JCPDS 29-0497) phases as revealed by XRD analysis (Fig. 8(a)). The morphology appears to be irregular grains of varying sizes (Fig. 8(b)). EDX analysis shows that the film is composed of Co (24%), P (33%), Se (43%).

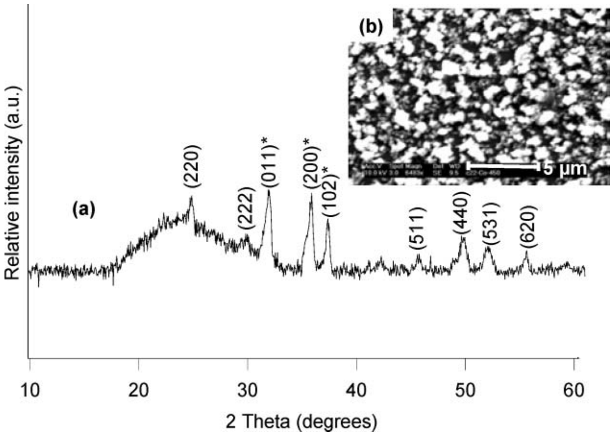

Fig. 8 XRD pattern (a) and SEM image (b) of a mixture of cobalt selenide and cobalt phosphide films deposited on glass from $[Co(Se_2P^iPr_2)_2]$ at 450 °C. "*" CoP peaks.

Deposition of nickel and cobalt selenide films from selenocarbamato precursors by AA-MOCVD

Preliminary AA-MOCVD studies from the selenocarbamato precursors deposited the corresponding metal selenide films. Nickel selenide films were deposited from $[Ni(Se_2CNEt_2)_2]$ (**5**) at 400 and 450 °C. SEM revealed the morphology (Fig. 9(a)) as irregular plates with size ranges from 1 to 2 µm for films deposited at 450 °C, whereas at 400 °C intertwined wires were observed (Fig. 10(c)). EDX indicated nickel deficient films with a 1 : 2 ratio of nickel to selenium, the cubic $NiSe_2$ phase (JCPDS 11-0552) being confirmed by XRD measurements. Cobalt selenide films were deposited from $[Co(Se_2CNEt_2)_3]$ (**6**) at 450 °C. XRD patterns of the films matched with the cubic $CoSe_2$ (JCPDS 09-0234) and the morphology of the film appears to be bundled fibres (Fig. 9(b). The elemental composition suggested by EDX matched with the expected Co : Se ratio of 1 : 2.

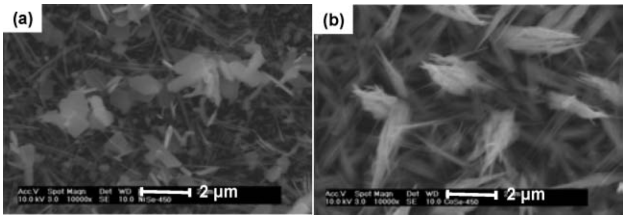

Fig. 9 SEM images of (a) nickel selenide films and (b) cobalt selenide films deposited on glass from $[Ni(Se_2CNEt_2)_2]$ and $[Co(Se_2CNEt_2)_3]$ at 450 °C.

Deposition behaviour of imidoselenophosphinato-, selenophosphinato- and selenocarbamato-metal complexes

Nickel selenide films deposited from imidoselenophosphinato, selenophosphinato and selenocarbamato precursors showed interesting features in their morphology, as studied by SEM under similar deposition conditions (400 °C). Fibrous material was deposited from the imidoselenophosphinato precursor (Fig. 10(a)) whereas spherical particles connected by wires were deposited from selenophosphinato precursor (Fig. 10(b)) and intertwined wires were deposited from the selenocarbamato precursor (Fig. 10(c)). $[Ni\{(SeP^iPr_2)_2N\}_2]$ and $[Ni(Se_2P^iPr_2)_2]$ deposited hexagonal $Ni_{0.85}Se$ films with preferred orientation along the (101) direction whereas $[Ni(Se_2CNEt_2)_2]$ gave a cubic $NiSe_2$ phase.

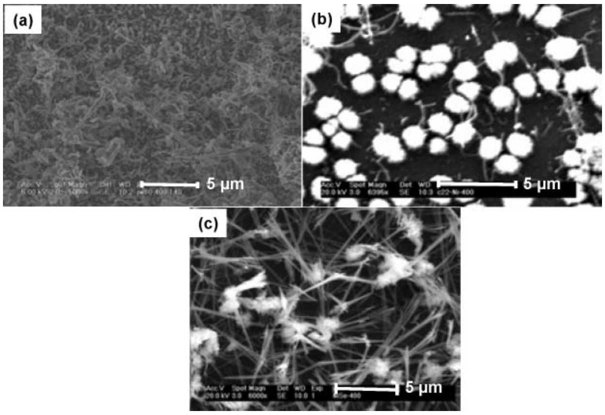

Fig. 10 SEM images of nickel selenide films deposited from (a) $[Ni\{(SeP^iPr_2)_2N\}_2]$, (b) $[Ni(Se_2P^iPr_2)_2]$ and (c) $[Ni(Se_2CNEt_2)_2]$ deposited at 400 °C.

The morphology of the cobalt selenide films deposited at 450 °C from the imidoselenophosphinato precursor showed a mixture of flakes and stacked rods (Fig. 11(a)). Irregular shaped particles composed of a mixture of cobalt selenide and cobalt phosphide were formed from the selenophosphinato precursor (Fig. 11(b)), whereas the selenocarbamato precursor yielded bundled fibres of cobalt selenide (Fig. 11(c)). $[Co\{(SeP^iPr_2)_2N\}_2]$ deposited cobalt selenide films at lower temperatures of 425 °C and 450 °C. Thin films of cobalt phosphide and cobalt selenide were deposited at higher temperatures of 475 °C and 525 °C, depending upon the position of the substrate in the reactor. XRD of the as-deposited

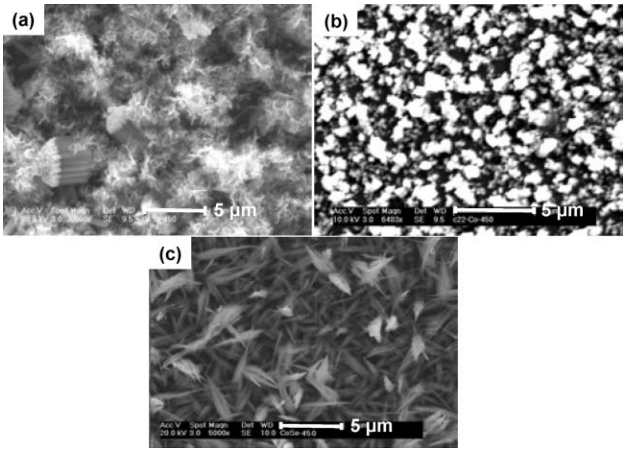

Fig. 11 SEM images of cobalt selenide films deposited from (a) $[Co\{(SeP^iPr_2)_2N\}_2]$, (b) $[Co(Se_2P^iPr_2)_2]$ and (c) $[Co(Se_2CNEt_2)_3]$ deposited at 450 °C.

cobalt selenide films at 525–425 °C showed the phase composition as orthorhombic $CoSe_2$ and cubic Co_3Se_4 with the preferred orientation along the (111) plane, whereas XRD of cobalt phosphide films grown at 525 °C and 475 °C correspond to monoclinic CoP_2 and orthorhombic CoP. $[Co(Se_2P^iPr_2)_2]$ produced a mixture of Co_9Se_8 and CoP films at 450 °C irrespective of the position of the substrate whereas $[Co(Se_2CNEt_2)_3]$ deposited only $CoSe_2$ films at 450 °C.

Experimental

All reagents were purchased from Sigma-Aldrich chemical company and used as received. Solvents were distilled prior to use. ^{1}H NMR studies were carried out using a Bruker AC300 FTNMR instrument. Mass spectra were recorded on a Micromass Trio 2000 instrument. Infrared spectra were recorded on a Specac single reflectance ATR instrument (4000–400 cm^{-1}, resolution 4 cm^{-1}). Elemental analysis was performed by the University of Manchester micro-analytical laboratory. TGA measurements were carried out by a Seiko SSC/S200 model under a heating rate of 10 °C min^{-1} under nitrogen. Melting point was recorded on a Stuart melting point apparatus and uncorrected. DSC measurements were performed on a Rheometric Scientific STA 1500H instrument.

Synthesis

The ligands $[^iPr_2P(Se)NHP(Se)^iPr_2]$[22] and $[(^iPr_2PSe_2)\ (HNEt_3)]$[45] and the complexes $[Co\{(SeP^iPr_2)_2N\}_2]$,[35] $[Ni(Se_2CNEt_2)_2]$[46a,b] and $[Co(Se_2CNEt_2)_3]$[46c] were prepared according to the published procedures.

$[Ni\{(SeP^iPr_2)_2N\}_2]$ (1). In a typical experiment, sodium methoxide (0.53 g, 10 mmol) was added to a stirred solution of $(SeP^iPr_2)_2NH$ (4.0 g, 10 mmol) in anhydrous methanol (100 cm^3). The resulting pink solution was stirred at room temperature for 10 min. Nickel(II) chloride hexahydrate (1.19 g, 5 mmol) was added and the reaction stirred at room temperature for 2 h. The resulting suspension was filtered and the recovered solid washed with methanol (100 cm^3) before drying under vacuum. The crude product was recrystallised from THF (40 ml) to give a red powder, yield (3.9 g, 93%). MS (EI/CI), m/z = [M$^+$] 871, $[Ni(SeP^iPr_2)_2N]$ 465, $[(SeP^iPr_2)_2N]$ 406; mp 190–192 °C. Elemental analysis (Found: C, 33.0; H, 6.2; N, 3.0; P, 13.8%, Calc. for $C_{24}H_{56}N_2Se_4P_4Ni$: C, 33.1; H, 6.5; N, 3.2; P, 14.2%). The red powder on recrystallisation at low temperature (4 °C) predominantly produced 80% green crystals with 20% red crystals.

$[Ni(Se_2P^iPr_2)_2]$ (2). In a typical experiment, a solution of nickel(II) chloride hexahydrate (1.19 g, 5 mmol) in 5 ml MeOH was added drop-wise to a solution of $(HNEt_3)(^iPr_2PSe_2)$ (3.77 g, 10 mmol) in 100 ml of MeOH. The mixture was stirred for 1 h at room temperature under atmospheric pressure forming a green precipitate, which was filtered off, washed with MeOH and recrystallised in dichloromethane (35 ml) to obtain green crystals, yield (2.58 g, 85%). MS (EI/CI), m/z = [M$^+$] 608, $[(Se_2P^iPr_2)]$ 275; mp 210–212 °C. Elemental analysis (Found: C, 23.8; H, 4.5; P, 10.6; Ni, 9.4. Calc. for $C_{12}H_{28}P_2Se_4Ni$: C, 23.7; H, 4.6; P, 10.2; Ni, 9.6%); ^{1}H NMR, δ(300 MHz; $CDCl_3$; Me_4Si) 1.43 (dd, 24H, $^3J_{HH}$ = 6.7 Hz, $^3J_{Ph}$ = 19.9 Hz, 4 × $CH(CH_3)_2$), 2.07 (dsep, 4H, $^3J_{HH}$ = 6.7 Hz, $^3J_{Ph}$ = 5.3 Hz, 4× $CH(CH_3)_2$). ^{31}P NMR, δ(162 MHz; $CDCl_3$) 80.93 ($^1J_{PSe}$ = 4.55 Hz).

$[Co(Se_2P^iPr_2)_2]$ (4). A similar procedure to (**2**) was carried out using cobalt(II) chloride hexahydrate (1.19 g, 5 mmol) to obtain a green powder. Recrystallisation from dichloromethane (40 ml) gave green crystals. Yield (2.65 g, 87%). MS (EI/CI), m/z = [M$^+$] 609, $[(Se_2P^iPr_2)]$ 275; mp 121–123 °C. Elemental analysis (Found: C, 22.4; H, 4.4; P, 10.3; Co, 8.8. Calc. for $C_{12}H_{28}P_2Se_4Co$: C, 23.6; H, 4.4; P, 10.2; Co, 9.7%).

X-Ray crystallography

Single-crystal X-ray diffraction data for the compounds were collected using graphite monochromated Mo-Kα radiation (λ = 0.71073 Å) on a Bruker APEX diffractometer. The structure was solved by direct methods and refined by full-matrix least squares on F^2.[47] All non-H atoms were refined anisotropically. H atoms were included in calculated positions, assigned isotropic thermal parameters and allowed to ride on their parent carbon atoms. All calculations were carried out using the SHELXTL package.[48]

CCDC reference numbers: 676882 (**1a**), 675796 (**1b**) and 675797 (**2**).

Deposition of films by AA-MOCVD

In a typical deposition, 0.20 g of the precursor was dissolved in 20 ml toluene in a two-necked 100 ml round-bottom flask with a gas inlet that allowed the carrier gas (argon) to pass into the solution to aid the transport of the aerosol. This flask was connected to the reactor tube by a piece of reinforced tubing. The argon flow rate of 160 sccm was used for deposition studies which was controlled by a Platon flow gauge. Seven glass substrates (approx. 1 × 3 cm) were placed inside the reactor tube, which is placed in a Carbolite furnace. The precursor solution in a round-bottom flask was kept in a water bath above the piezoelectric modulator of a PIFCO ultrasonic humidifier (Model No. 1077). The aerosol droplets of the precursor thus generated were transferred into the hot-wall zone of the reactor by carrier gas. Both the solvent and the precursor were evaporated and the precursor vapour reached the heated substrate surface where thermally induced reactions and film deposition took place.

Table 2 Selected crystal data and refinement parameters for (**1**) and (**2**)

	$[Ni\{(SeP^iPr_2)_2N\}_2]$		$[Ni(Se_2P^iPr_2)_2]$
	Square planar	Tetrahedral	Square planar
Empirical formula	$C_{24}H_{56.63}NiN_2O_{0.31}P_4Se_4$	$C_{24}H_{56}NiN_2P_4Se_4$	$C_{12}H_{28}NiP_2Se_4$
Formula weight	876.82	871.14	608.83
Temperature/K	100(2)	100(2)	100(2)
Crystal system	Monoclinic	Triclinic	Monoclinic
Space group	$C2/c$	$P\bar{1}$	$P2(1)/n$
a/Å	13.254(4)	9.289(1)	9.287(1)
b/Å	21.292(4)	12.913(2)	10.935(1)
c/Å	13.585(3)	16.302(2)	10.136(1)
α/°	90	79.058(2)	90
β/°	112.961(5)	78.221(2)	97.904(2)
γ/°	90	69.895(2)	90
V/Å^3	3530.2(1)	1782.3(4)	1019.5(2)
Z	4	2	2
Density (calculated)/Mg m^{-3}	1.650	1.623	1.983
Absorption coefficient/mm^{-1}	4.874	4.285	8.236
F(000)	1765	876	588
Crystal size/mm	0.20 × 0.20 × 0.03	0.20 × 0.20 × 0.03	0.55 × 0.55 × 0.50
θ range for data collection/°	1.91 to 28.35	1.29 to 27.10	2.75 to 26.37
Limiting indices	$-13 \le h \le 17, -28 \le k \le 21, -17 \le l \le 16$	$-11 \le h \le 11, -16 \le k \le 15, -20 \le l \le 20$	$-11 \le h \le 9, 13 \le k \le 13, -10 \le l \le 12$
Reflections collected	11098	14856	5643
Unique reflections	4153 [R(int) = 0.0444]	7664 [R(int) = 0.0415]	2067 [R(int) = 0.0216]
Completeness to θ (%)	($\theta = 28.35°$) 94.1	($\theta = 27.10°$) 97.4	($\theta = 26.37°$) 99.4
Max. and min. transmission	0.8676 and 0.4424	0.8688 and 0.4453	0.1045 and 0.0929
Refinement method	Full-matrix least-squares on F^2	Full-matrix least-squares on F^2	Full-matrix least-squares on F^2
Data/restraints/parameters	4153/0/170	7664/0/332	2067/0/92
Goodness-of-fit on F^2	0.983	1.074	1.074
Final R indices [$I > 2\sigma(I)$]	$R1 = 0.0356$, $wR2 = 0.0680$	$R1 = 0.0475$, $wR2 = 0.0995$	$R1 = 0.0198$, $wR2 = 0.0470$
R indices (all data)	$R1 = 0.0577$, $wR2 = 0.0747$	$R1 = 0.0637$, $wR2 = 0.1051$	$R1 = 0.0224$, $wR2 = 0.0479$
Largest diff. peak and hole/e Å^{-3}	0.667 and −0.469	0.959 and −0.576	0.543 and −0.446

Characterisation of thin films

X-Ray diffraction studies were performed on a Bruker AXS D8 diffractometer using Cu-K$_\alpha$ radiation. The samples were mounted flat and scanned between 10 and 70° in a step size of 0.05° with a count rate of 9 s. Films were carbon coated using Edward's E306A coating system before carrying out SEM and EDX analyses. SEM analysis was performed using a Philips XL 30FEG and EDX was carried out using a DX4 instrument.

Conclusions

The X-ray structure of $[Ni\{(SeP^iPr_2)_2N\}_2]$ (**1**) revealed that the compound is square planar in the green and tetrahedral in the red crystals. This behaviour of $[Ni\{(SeP^iPr_2)_2N\}_2]$ seems to be unique in the class of imidodichalcogenidophosphinato derivatives. Nickel selenide films were deposited from all three classes of compounds [(**1**), (**2**) and (**5**)] but the morphology of the films varied depending on the coordinating ligand. In the case of cobalt, the selenocarbamato precursor (**6**) behaved similarly to the corresponding nickel complex (**5**) and gave only cobalt selenide films. But the selenophosphinato- and imidoselenophosphinato-cobalt(II) precursors deposited different types of material when compared to the nickel complexes. The selenophosphinato-cobalt precursor (**4**) yielded a mixture of cobalt selenide and cobalt phosphide films whereas the imidodiselenodiphosphinato-cobalt precursor (**3**) produced two types of film, cobalt selenide and cobalt phosphide at higher deposition temperatures (525 and 475 °C). The reason for this behaviour may be due to the large E···E "bite" (*ca.* 4 Å) of the imidodiselenophosphinate ligand inducing less strain on the metal–ligand ring.[49] The Co–Se bond length (2.435 Å)[35] in (**3**) is longer than Ni–Se bond length (2.400 Å) in (**1**), so bond cleavage is more susceptible in (**3**) at higher temperatures and hence it deposited cobalt selenide and cobalt phosphide films.

Acknowledgements

A. P. is thankful to The University of Manchester for OSS funding. C. Q. N. would like to acknowledge the Government of Vietnam for financial support. The authors also thank EPSRC, UK for grants to P. O'B. that have made some of this research possible.

Notes and references

1 M. Bonamico, G. Mazzone, A. Vaciago and I. Zambonelli, *Acta Crystallogr.*, 1965, **19**, 898.
2 A. Saunders, A. Vecht and G. Tyrell, *Proceedings of the 7th International Conference on Ternary Multiary Compounds (1986)*, Materials Research Society, Pittsburgh, PA, 1987 (*Chem. Abstr.*, 1988, **108**, 666226h).
3 B. L. Druz, Y. N. Eutukhov and M. Y. Rakhlin, *Metalloorg. Khim.*, 1988, **1**, 357 (*Organomet. Chem. USSR*, 1988, **1**, 357).
4 D. M. Frigo, O. F. Z. Khan and P. O'Brien, *J. Cryst. Growth*, 1989, **96**, 989.
5 M. B. Hursthouse, M. A. Malik, M. Motevalli and P. O'Brien, *Polyhedron*, 1992, **11**, 45.
6 R. D. Pike, H. Cui, R. Kershaw, K. Dwight, A. Wold, T. N. Blanton, A. A. Wernberg and H. J. Gysling, *Thin Solid Films*, 1993, **224**, 221.

7 P. O'Brien, J. R. Walsh, I. M. Watson, L. Hart and S. R. P. Silva, *J. Cryst. Growth*, 1996, **167**, 133.

8 P. O'Brien, J. R. Walsh, I. M. Watson, M. Motevalli and L. Henrikson, *J. Chem. Soc., Dalton Trans.*, 1996, 2491.

9 T. Trindade and P. O'Brien, *J. Mater. Chem.*, 1996, **6**, 343.

10 M. Afzaal, D. Crouch, M. A. Malik, M. Motevalli, P. O'Brien and J.-H. Park, *J. Mater. Chem.*, 2003, **13**, 639.

11 (*a*) F. Srouji, M. Afzaal, J. Waters and P. O'Brien, *Chem. Vap. Deposition*, 2005, **11**, 91; (*b*) G. Hogarth, *Prog. Inorg. Chem.*, 2005, **53**, 71.

12 P. O'Brien and J. Waters, *Chem. Vap. Deposition*, 2006, **12**, 620.

13 J. H. Park, M. Afzaal, M. Helliwell, M. A. Malik, P. O'Brien and J. Raftery, *Chem. Mater.*, 2003, **15**, 4205.

14 M. Afzaal, D. J. Crouch, P. O'Brien, J. Raftery, P. J. Skabara, A. J. P. White and D. J. Williams, *J. Mater. Chem.*, 2004, **14**, 233.

15 M. Afzaal, D. Crouch, M. A. Malik, M. Motevalli, P. O'Brien, J. -H. Park and J. D. Woollins, *Eur. J. Inorg. Chem.*, 2004, 171.

16 (*a*) S. S. Garje, J. S. Ritch, D. J. Eisler, M. Afzaal, P. O'Brien and T. Chivers, *J. Am. Chem. Soc.*, 2006, **128**, 3120; (*b*) M. C. Copsey, A. Panneerselvam, M. Afzaal, T. Chivers and P. O'Brien, *Dalton Trans.*, 2007, 1528.

17 C. Q. Nguyen, A. Adeogun, M. Afzaal, M. A. Malik and P. O'Brien, *Chem. Commun.*, 2006, 2179.

18 C. Q. Nguyen, A. Adeogun, M. Afzaal, M. A. Malik and P. O'Brien, *Chem. Commun.*, 2006, 2182.

19 (*a*) M. A. Malik, M. M. Zulu, P. O'Brien and G. Wakefield, *J. Mater. Chem.*, 1998, **8**, 1885; (*b*) B. Ludolph, M. A. Malik, P. O'Brien and N. Revaprasadu, *Chem. Commun.*, 1998, 1849.

20 F. T. Wang, J. Najdzionek, K. L. Leneker, H. Wasserman and D. Braitsch, *Synth. React. Inorg. Met.-Org. Chem.*, 1978, **8**, 119.

21 A. Schmidpeter, R. Böhm and M. H. Groeger, *Angew. Chem.*, 1964, **3**, 704.

22 D. Cupertino, D. J. Birdsall, A. M. Z. Slawin and J. D. Woollins, *Inorg. Chim. Acta*, 1999, **290**, 1.

23 C. Papadimitriou, P. Veltsistas, J. Novosad, R. Cea-Olivares, A. Toscano, P. Garcia, Y. Garcia, M. L. Cardosa, A. M. Z. Slawin and J. D. Woollins, *Polyhedron*, 1997, **16**, 2727.

24 D. J. Birdsall, A. M. Z. Slawin and J. D. Woollins, *Polyhedron*, 2001, **20**, 125.

25 D. Cupertino, R. W. Keyte, A. M. Z. Slawin and J. D. Woollins, *Polyhedron*, 1999, **18**, 707.

26 I. P. Gray, A. M. Z. Slawin and J. D. Woollins, *Dalton Trans.*, 2005, 2188.

27 T. Q. Ly and J. D. Woollins, *Coord. Chem. Rev.*, 1998, **176**, 451.

28 W. Kuchen, J. Metten and A. Judat, *Chem. Ber.*, 1964, **97**, 2306.

29 W. Kuchen and B. Knop, *Angew. Chem., Int. Ed. Engl.*, 1965, **4**, 244.

30 W. Kuchen and H. Hertel, *Angew. Chem., Int. Ed. Engl.*, 1969, **8**, 89.

31 M. Afzaal, S. M. Aucott, D. Crouch, P. O'Brien, J. D. Woollins and J. -H. Park, *Chem. Vap. Deposition*, 2002, **8**, 187.

32 M. Afzaal, D. Crouch, P. O'Brien and J. -H. Park, *J. Mater. Sci.: Mater. Electron.*, 2003, **14**, 555.

33 M. Afzaal, K. Ellwood, N. L. Pickett, P. O'Brien, J. Raftery and J. Waters, *J. Mater. Chem.*, 2004, **14**, 1310.

34 S. S. Garje, J. S. Ritch, D. J. Eisler, M. Afzaal, P. O'Brien and T. Chivers, *J. Mater. Chem.*, 2006, **16**, 966.

35 L. M. Gilby and B. Piggot, *Polyhedron*, 1999, **18**, 1077.

36 I. Lifschitz, J. G. Bos and K. M. Dijkema, *Z. Anorg. Allg. Chem.*, 1939, **242**, 97.

37 I. Lifschitz and J. G. Bos, *Recl. Trav. Chim. Pays-Bas*, 1940, **59**, 407.

38 I. Lifschitz and K. M. Dijkema, *Recl. Trav. Chim. Pays-Bas*, 1941, **60**, 581.

39 M. R. Churchill, J. Cooke, J. P. Fennessey and J. Wormald, *Inorg. Chem.*, 1971, **10**, 1031.

40 P. Bhattacharyya, J. Novosad, J. Phillips, A. M. Z. Slawin, D. J. Williams and J. D. Woollins, *J. Chem. Soc., Dalton Trans.*, 1995, 1607.

41 D. Cupertino, R. Keyte, A. M. Z. Slawin, D. J. Williams and J. D. Woollins, *Inorg. Chem.*, 1996, **35**, 2695.

42 R. Rosler, C. Silvestru, G. Espinosa-Perez, I. Haiduc and R. Cea-Olivares, *Inorg. Chim. Acta*, 1996, **241**, 47.

43 E. Simon-Manso, M. Valderramma and D. Boys, *Inorg. Chem.*, 2001, **40**, 3647.

44 J. H. Zhan, X. G. Yang, S. D. Li, Y. Xie, W. C. Yu and Y. T. Qian, *J. Solid State Chem.*, 2000, **152**, 537.

45 C. Q. Nguyen, M. Afzaal, M. A. Malik, M. Helliwell, J. Raftery and P. O'Brien, *J. Organomet. Chem.*, 2007, **692**, 2669.

46 (*a*) M. Bonamicco and G. Dessy, *Chem. Commun. (London)*, 1967, 1114; (*b*) C. Furlani, E. Cervone and F. D. Camassei, *Inorg. Chem.*, 1968, **7**, 265; (*c*) W. Dietzsch, N. V. Duffy, A. M. Lee, B. W. Skelton and A. H. White, *Z. Anorg. Allg. Chem.*, 2006, **632**, 2419.

47 G. M. Sheldrick, *SHELXS-97 and SHELXL-97*, University of Göttingen, Germany, 1997.

48 *Bruker, SHELXTL Version 6.12*, Bruker AXS Inc., Madison, Wisconsin, USA, 2001.

49 (*a*) J. D. Woollins, *J. Chem. Soc., Dalton Trans.*, 1996, 2893; (*b*) D. Maganas, S. S. Staniland, A. Grigoropoulos, F. White, S. Parsons, P. Kyritsis and G. Pneumatikakis, *Dalton Trans.*, 2006, 2301.